

# Analytical Model for Simulation of Forming Process & Residual Stresses in Helical Springs

## — Part 1

by:

Dr.-Ing. Vladimir Kobelev  
Mühr und Bender KG  
P.O. 360  
D-57427, Attendorn, Germany  
www.mubea.com

**Residual stress can have a great effect on the properties of a material. This article offers a mathematical theory of residual stresses and strains in helical springs that allows calculating stresses on all manufacturing process steps, particularly during coiling and presetting.**

*In Part 1 of this article, the author looks at the Isotropic Work-Hardening Stress-Strain Law and the theory of elastic-plastic combined bending and torsion of a naturally curved and twisted bar. Complete mathematical analyses are provided.*

Residual stresses remain after the original cause of the stresses (in-service forces, heat gradient) has been removed<sup>1,2</sup>. Residual stress also exists in the bulk of a material without application of an in-service load (applied force, displacement of thermal gradient). They remain along a cross section of the component, even without the external cause. Residual stresses occur for a variety of reasons, including inelastic deformations and heat treatment.

Heat from welding may cause localized expansion, which is taken up during welding by either the molten metal or the placement of parts being welded. When the finished weldment cools, some areas cool and contract more than others, leaving residual stresses.

While uncontrolled residual stresses are undesirable, many designs rely on them. For example, toughened glass and pre-stressed concrete depend on them to prevent brittle failure. Similarly, a gradient in martensite formation leaves residual stress that can prevent the opening of edge cracks. Other examples of residual stress are shot peening and presetting stresses.

Shot peening is widely used as a mechanical surface treatment for many components such as crankshafts, gears, springs, etc. During the shot

peening, process steel, glass or ceramic balls are projected to the surface of the material with a high speed. This leads to a plastic deformation of the surface layers. To keep the cohesion between the stretched surface and the core, these layers are then set to overwhelmingly compressive stresses. These compressions are compensated by tensile stresses in the bulk of the sample.

Usually, compressive residual stress has a beneficial effect on fatigue life and stress corrosion as it delays crack initiation and propagation. Tensile stress on the contrary reduces mechanical performance of materials. In the elastic range, residual stress can just be added to the applied stress as a static load. For this reason, compression can allow reduction of the stress level of the layers where the applied load is the highest. This leads to an apparent increase of the fatigue limit.

In the case of cyclic loading, cracks can initiate and propagate for a stress level much lower than the yield strength. This leads to redistribution (relaxation) of the residual stress. An accommodation of the structure to the applied load takes place. It has to be pointed out that compressive residual stress leads to crack closure and therefore delays crack propagation.

Residual stresses are also produced by heterogeneous plastic deformations, thermal contractions and phase transformations induced by the manufacturing process. A common intentional use of residual stress is in press fits.

Depending on the scale at which the matter is analyzed, different kinds of stresses are classically defined. Three kinds of residual stresses are usually defined as macro stresses (or stresses of first kind)

over a few grains, stresses of a second kind over one particular grain and stresses of a third kind across sub-microscopic areas (several atomic distances within a grain). The second and third stress types are also called micro stresses.

In this section we study an important practical problem of residual stresses in helical springs. We demonstrate the possibility of the creation of residual stress on the surface of helical springs and compare the theoretically optimal distribution of stresses and the residual stresses resulting from modern manufacturing technology.

Helical compression springs for automotive suspensions are formed either by coiling wire at ambient conditions (cold coil) or by coiling wire that is at red heat (hot coil)<sup>3, 4, 5</sup>.

In the hot coiling process, cut wire segments of steel are heated above the austenitizing temperature and fed directly onto a mandrel that rapidly forms the coil. The formed coil is quenched and later tempered well below the austenitizing temperature. The springs are preset with torsion residual stress by compression to solid height (bulldozing) and shot peened.

The primary disadvantages of the hot coiling process are a risk of decarburization and scaling of the wire surface. Scaling is detrimental to the fatigue performance of the spring, since it results in crack initiation sites on the surface. In cold coiling, wire is fed from a spool onto a mandrel at room-temperature to form the coil. The formed and cut coils are then stress relieved in a furnace, bulldozed and shot peened. Since stress relieving is done at temperatures well below the austenitizing temperature, decarburization and surface scaling are avoided.

As a consequence, wire for cold coiled springs can be specified with a higher quality surface finish and a smaller diameter than a similar spring manufactured by the hot coiling process. When a helical compression spring is loaded in service, its overall height is reduced.

Within the wire itself, the bulk of the deformation that is necessary to make this happen is pure torsion. The torsion is uniform throughout the length of the coiled wire. Depending on end effects at the top and bottom of a helical spring, in addi-

tion to torsion, a minor bending moment may be introduced.

Any residual stresses are additive with these load stresses. Their addition can be either harmful or beneficial, depending on relative sign and magnitude. The following three examples are significant to the processing of helical springs (see **Table 1**).

**Table 1: Examples of Residual Stress**

- Coiling process itself introduces residual stresses known to be detrimental to fatigue and corrosion properties.
- Presetting a spring by bulldozing causes yielding. On release, the surface is left with a residual shear stress site in sign to in-service load stress—improving the fatigue properties.
- Shot-peening introduces uniform compressive stresses at the surface of the wire and is known to noticeably amplify the fatigue resistance of springs, particularly when it is applied after bulldozing.

Because the stress relieving anneal can also degrade the temper of the wire, complete elimination of residual coiling stresses is not necessarily desirable. Similarly, excessive shot peening intensity can lead to a degradation of fatigue resistance.

Stress management in springs is therefore an optimization of factors including the stress relief temperature, the wire strength, the shot peening intensity and the presetting conditions. Knowledge of how individual processing steps influence the residual coiling stresses is a necessary step in the process toward achieving a proper optimization of residual stresses.

In this article, we apply the deformation theory of plasticity, where the stress tensor is a function of the strain tensor<sup>6, 7, 8</sup>. The deformation theory of plasticity could be applied in problems of proportional or simple loading, in which all stress components increase proportionally.

According to this theory, we assume the stress-strain law for the active plastic deformation of the medium. The mathematical analysis for this is seen in **Table 2**.

## Analytical Model for Simulation of Forming Process ...continued

**Table 2 — The Isotropic Work-Hardening Stress-Strain Law.**

In this article we apply the deformation theory of plasticity, where the stress tensor is a function of the strain tensor [1, 2, 3]. The deformation theory of plasticity could be applied in problems of proportional or simple loading, in which all stress components increase proportionally. According to this theory, we assume the following stress-strain law for the active plastic deformation of the medium:

$$(2.1) \quad \mathbf{s} = 2G_p(\Gamma^2)\mathbf{e}, \quad \boldsymbol{\varepsilon} = \boldsymbol{\sigma} / K,$$

$$(2.2) \quad \mathbf{s} = \begin{bmatrix} s_{xx} & \tau_{xy} & \tau_{xz} \\ \tau_{xy} & s_{yy} & \tau_{yz} \\ \tau_{xz} & \tau_{yz} & s_{zz} \end{bmatrix}, \quad \mathbf{e} = \begin{bmatrix} e_{xx} & \varepsilon_{xy} & \varepsilon_{xz} \\ \varepsilon_{xy} & e_{yy} & \varepsilon_{yz} \\ \varepsilon_{xz} & \varepsilon_{yz} & e_{zz} \end{bmatrix} = \begin{bmatrix} e_{xx} & \gamma_{xy}/2 & \gamma_{xz}/2 \\ \gamma_{xy}/2 & e_{yy} & \gamma_{yz}/2 \\ \gamma_{xz}/2 & \gamma_{yz}/2 & e_{zz} \end{bmatrix},$$

$$(2.3) \quad \Gamma^2 = \frac{2}{3} \left[ (\varepsilon_x - \varepsilon_y)^2 + (\varepsilon_y - \varepsilon_z)^2 + (\varepsilon_z - \varepsilon_x)^2 + \frac{3}{2} (\gamma_{xy}^2 + \gamma_{yz}^2 + \gamma_{xz}^2) \right],$$

$$(2.4) \quad \boldsymbol{\varepsilon} = \varepsilon_{xx} + \varepsilon_{yy} + \varepsilon_{zz} = Sp\boldsymbol{\varepsilon}, \quad \boldsymbol{\sigma} = \sigma_{xx} + \sigma_{yy} + \sigma_{zz} = Sp\boldsymbol{\sigma}.$$

The scalar invariant  $\Gamma$  represents the intensity of shear strain. The constant  $K$  is the bulk modulus. In the Equations (51)-(53) instead of stress  $\boldsymbol{\sigma}$  and strain  $\boldsymbol{\varepsilon}$  tensors we use the deviatoric stress tensor  $\mathbf{s}$  and the deviatoric strain tensor  $\mathbf{e}$ :

$$\begin{aligned} s_{xx} &= \sigma_{xx} - \sigma/3, & s_{yy} &= \sigma_{yy} - \sigma/3, & s_{zz} &= \sigma_{zz} - \sigma/3, \\ e_{xx} &= \varepsilon_{xx} - \varepsilon/3, & e_{yy} &= \varepsilon_{yy} - \varepsilon/3, & e_{zz} &= \varepsilon_{zz} - \varepsilon/3. \end{aligned}$$

Similarly, the scalar invariant  $T$  represents the intensity of shear stresses

$$(2.5) \quad T^2 = \frac{2}{3} \left[ (\sigma_x - \sigma_y)^2 + (\sigma_y - \sigma_z)^2 + (\sigma_z - \sigma_x)^2 + 6(\tau_{xy}^2 + \tau_{yz}^2 + \tau_{xz}^2) \right].$$

With these equations the dependence of stress intensity is the certain function of strain intensity:  $T = G_p(\Gamma^2)\Gamma$ .

For the linear elastic isotropic Material the dependence of stress intensity of strain intensity is linear:  $T = G_0\Gamma$ .

The only material constant in this equation is the shear modulus  $G_0$ . The bulk modulus  $K = 2G_0(1+\nu)/(3-6\nu)$  relates to the shear modulus in linear elastic region. The Poisson's ratio  $\nu$  is assumed to be constant over the deformation history.

The actively deformed plastic medium could be characterized by the empiric function (5.6) with the secant modulus  $G_p(\Gamma^2)$ .

The inversion of the relation (2.6) reads:  $\Gamma = F_p(T^2)\Gamma$ .

In our Model we postulate the following dependence of the secant modulus upon the intensity of shear strain  $\Gamma$ :

$$(2.6) \quad G_p(\Gamma^2) = \frac{G_0}{\sqrt{1 + \frac{\Gamma^2}{\varepsilon_p^2}}}, \quad F_p(T^2) = \frac{1}{G_p(\Gamma^2)} = \frac{G_0^{-1}}{\sqrt{1 - \frac{T^2}{\sigma_p^2}}}$$

with  $\sigma_p = G_0\varepsilon_p$ . During the unload process the material demonstrates the linear elastic behavior with the initial shear modulus  $G_0$ .

Use of stress-strain relations instead of the stress-strain-rate relations is theoretically admissible, if the former can be obtained from the latter by path-independent integration [4]. One possible case of proportional or "radial" loading with fixed stress-axes and principal strain ratios is considered in this Article. The simplification of the solutions of boundary value problems through the use of stress-strain relations instead of stress-strain-rate relations is considerable. From the physical point of view it seems preferable to obtain an analytic solution in closed form than a rigorous that can be evaluated for specific conditions by elaborate numerical methods.

The expressions (2.7) could be generalized, allowing more approximation constants for more adequate material descriptions. For a compressible isotropic work-hardening material, without the distinct yielding point, as observed in the behavior of deformation, the following stress strain expressions could be applied. The following generalized dependence of secant modulus upon deviatoric strain reads:

$$(2.7) \quad G_p = G_\infty + \left[ 1 + \frac{\varepsilon_{zz}^2 + \omega^2 \varepsilon_{xz}^2 + \omega^2 \varepsilon_{yz}^2}{\varepsilon_p^2} \right]^{-k} (G_0 - G_\infty)$$

Here we use the following notations for the plastic yield strain  $\varepsilon_p$ , plastic yield stress  $\sigma_p = E\varepsilon_p$ , hardening exponent  $k$  and Young modulus  $E_0 = 2(1+\nu)G_0$  respectively.

For the considered stress state of combined bending and torsion of the rod we have  $\omega^2 = 3/(1+\nu)^2$ . The Poisson coefficient is assumed, as common, to be constant during the deformation history. The stress tensor reduces to

$$\boldsymbol{\sigma} = \begin{bmatrix} 0 & 0 & 2G_s\varepsilon_{xz} \\ 0 & 0 & 2G_s\varepsilon_{yz} \\ 2G_s\varepsilon_{xz} & 2G_s\varepsilon_{yz} & \frac{3EG_s}{E + (1-2\nu)G_s}\varepsilon_{zz} \end{bmatrix}.$$

Particularly, if the Poisson's ratio is  $\nu = 1/2$  we get  $E_p = 3G_p$ .

For positive values of  $k$  the secant modulus decreases, as it usually does for common metals and alloys. The limit value of stress for  $\mathcal{E} \rightarrow \infty$  and for  $k = 1/2$  is  $\sigma_p = E\mathcal{E}_p$ . At this limit for  $k = 1$  the stress vanishes. The secant modulus increases for negative values of  $k$ . This is typically for rubber or some synthetics.

The stress-strain relation (2.1) demonstrates remarkable properties. The experimental data from torsion could be approximated by (2.1) for a variety of structural materials. There are two distinct regions for secant modulus, namely the small strain region and large strain region. The initial secant modulus corresponds to the shear modulus of linear elasticity  $G_s \underset{I_2 \rightarrow 0}{\sim} G$ .

For the large strain the asymptotical behavior of secant modulus is  $G_s \underset{I_2 \rightarrow \infty}{\sim} G_\infty$ .

The stress-strain law was determined experimentally for steel 54CrSi6 (DIN 10089, Material number 1.7102). The standard probes of diameter  $d = 2r = 3.8 \text{ mm}$  were twisted to maximal value of twist rate per unit length of  $\theta = 0.35$ . The vector of torsion moment points  $M_n^{(T)}, n = 1..N$  was measured for different prescribed values of twist rate  $\theta_i, i = 1..N$ .

To determine the stress-strain curve we need the shear stress  $\tau_i, i = 1..N$  for each value of twist rate  $\theta_i, i = 1..N$ . For this purpose, we have to calculate backwards the shear stress vector from the vector of torsion moments. In other words, the inverse problem has to be solved. For this purpose, the method of piecewise linear approximation was implemented. With this piecewise linear approximation, the stress-strain curve was assumed in form

$$(2.8) \quad \tau(\gamma) = \tau_{i-1} + (\tau_i - \tau_{i-1}) \frac{\gamma - \gamma_{i-1}}{\gamma_i - \gamma_{i-1}} \quad \text{for } \gamma_{i-1} < \gamma \leq \gamma_i$$

The values of vector components for shear  $\gamma_i = r\theta_i, i = 1..N$  are immediately determined from the twist rates  $\theta_i$ . The values of vector components for shear stress  $\tau_i, i = 1..N$  are initially unknown variables and have to be determined from the acquired torsion moment data. The torque is the function of the twist rate per unit length  $\theta$ :

$$M^{(T)}(\theta) = 2\pi \int_0^r \tau(\rho\theta) \rho^2 d\rho.$$

Substitution of the piecewise linear approximation (2.9) for  $\tau(\gamma)$  in the above integral delivers the values of vector components for moment  $M_n^{(T)}, n = 1..N$  for each value of twist rate  $\gamma_i, i = 1..N$  in the following form

$$(2.9) \quad M_n^{(T)} = \frac{2\pi R^3}{\gamma_n} \sum_{i=1}^n \frac{1}{3} \left( \tau_{i-1} - \frac{\tau_i - \tau_{i-1}}{\gamma_i - \gamma_{i-1}} \gamma_{i-1} \right) (\gamma_i^3 - \gamma_{i-1}^3) + \frac{2\pi R^3}{\gamma_n} \sum_{i=1}^n \frac{1}{4} \left( \frac{\tau_i - \tau_{i-1}}{\gamma_i - \gamma_{i-1}} \right) (\gamma_i^4 - \gamma_{i-1}^4).$$

for  $1 < n < N$ .

The torque moments  $M_n^{(T)}$  were acquired for  $N$  initially prescribed acquisition points  $\gamma_i$ . To determine  $N$  unknown  $\tau_i$  the system of  $N$  linear algebraic equations (2.10) was solved. The matrix of the linear algebraic system (2.3) possesses the upper triangle form. This solution delivers the values of  $\tau_i, i = 1..N$  for the piecewise linear approximation (2.9) of the stress-strain law.

Our aim is to achieve a much simpler approximation of the form (2.8), which is much better suited for simulations than the piecewise linear approximation (2.9). Namely, we perform the plastic analysis of the combined bending and torsion with the stress-strain law (2.8), which is valid for an arbitrary Poisson coefficient  $\nu$ :

$$\tau_{rz} = \tau_{rz}(0, \gamma_{rz}) \equiv G_\infty \gamma_{rz} + (G_0 - G_\infty) \gamma_{rz} \left[ 1 + \omega^2 \left( \frac{\gamma_{rz}}{\mathcal{E}_p} \right)^2 \right]^{-k}$$

The magnitude of shear in this equation is  $\tau_{rz} = \sqrt{\tau_{xz}^2 + \tau_{yz}^2}$ .

We approximate namely the determined piecewise linear approximation (2.3) of the stress-strain law by the functional law. The least square approximation with functional law delivers the following values:

$$G_0 = 81.52 \text{ GPa}, E_0 = 204.45 \text{ GPa}, \sigma_p = 3.205 \text{ GPa}, \nu = 0.254, G_\infty = 0, k = 0.5.$$

With these values the following functional stress-strain law was obtained:

$$\tau_{rz}(0, \gamma_{rz}) = \frac{99947 \gamma_{rz}}{\sqrt{1 + 7426 \gamma_{rz}^2}}$$

From this shear-strain law we deduce immediately the functional stress-strain law. Applying the expression for hydrostatic stress, the non-vanishing components of stress tensor reduce to

$$(2.10) \quad \sigma_{zz}(\mathcal{E}_{zz}, \gamma_{rz}) = E_\infty \mathcal{E}_{zz} + (E_0 - E_\infty) \mathcal{E}_{zz} \left[ 1 + (\mathcal{E}_{zz}^2 + \omega^2 \gamma_{rz}^2) / \mathcal{E}_p^2 \right]^k,$$

$$\tau_{rz}(\mathcal{E}_{zz}, \gamma_{rz}) = G_\infty \gamma_{rz} + (G_0 - G_\infty) \gamma_{rz} \left[ 1 + (\mathcal{E}_{zz}^2 + \omega^2 \gamma_{rz}^2) / \mathcal{E}_p^2 \right]^k.$$

## Theory of Elastic-Plastic Combined Bending & Torsion of Naturally Curved & Twisted Bar

### Combined Bending & Torsion of a Bar, Loaded by a Terminal Bending Couple

In this article we study analytically the residual stresses due to coiling and presetting of helical springs. One coil of the cylindrical helical spring is shown in **Figure 1**.

The theory of elastic helical spring is provided in Sections 270, 271<sup>10</sup>. The residual stresses in helical compression spring could be determined analytically with the application of plasticity theory of combined torsion and bending of the naturally curved rod. The preset is applied to the helical compression spring by means of axial preset force and to the helical torsion spring by means of preset moment.

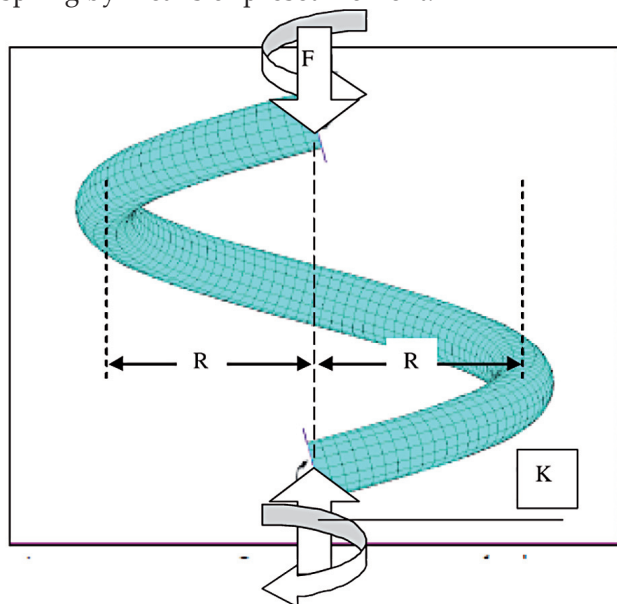


**Fig. 1** — One coil of the cylindrical helical spring under compression force  $F$  and twist moment  $K$ .

The elasto-plastic problem of combined bending and torsion of a straight prismatic bar, loaded by a terminal bending couple about the axis of symmetry of the cross section and a twisting couple problem was originally discussed by **Handelman**<sup>11</sup>. Assuming a **Levy-Mises** material, a nonlinear, partial differential equation was derived.

For steel bars of circular section plastically strained by combined bending and twisting couples in constant ratio, the moment-angle relations were reported<sup>12</sup>. The bending and twisting moments approach the theoretical values calculated for the fully plastic state of a plastic-rigid material. Very good

estimates of the latter values are obtained by bracketing between the upper and lower approximate values. A general relation is proposed between the fully plastic values of bending moment, torque and axial force when all three are applied together. This relation applies for a wide variety of sections and is suitable for plastic limit design.

A long prismatic member is acted upon by combinations of bending moments and torques of such a magnitude so as to render the member just fully plastic, was discussed<sup>13</sup>. The citing paper takes **Handelman's** equation and solves it numerically for a square section member. The stress distributions (shear and bending) are provided in a member for two critical combinations of moment and torque.

The **Reuss** equations are used<sup>14</sup> for analysis of particular combinations of twist and extension of a solid circular cylinder. The Reuss equations are integrated for different cases to give okastuic material shear stress and tension. A more general case, in which twist and extension are such as to make the ratio load to torque constant, is solved numerically. Finally the residual stresses are evaluated, after partial unloading, for a bar which has been twisted and extended in constant ratio.

Upper and lower approximations are obtained<sup>15</sup> to the interaction curve of the bending and twisting couples at yield for the combined bending and twisting of cylinders of ideally plastic-rigid material. Yield criteria expressed in the paper<sup>16</sup> in terms of stress resultants are obtained for typical engineering structures, using the first fundamental theorem of limit analysis. These yield criteria, which are often nonlinear, are then replaced by inscribed piece-wise linear approximations. The complete solutions based on these approximate yield criteria provide lower bounds; the corresponding values for the upper bound can be obtained by multiplying the lower bound values by a suitable factor.

The plastic flexure and torsion of prismatic beams was studied<sup>17</sup>. The prismatic bars are loaded by terminal bending and twisting moments which, acting together, cause full plastic flow. The material is assumed to behave according to the **Tresca-Levy-Mises** hypotheses, and in nonhardening and rigid plastic. The results were obtained by numerical solution of the second order nonlinear differential equation derived by **Handelman** for a **Levy-Mises** material, and the beam sections investigated were circular,

square and triangular. The relationships obtained were found to give points lying virtually on a single interaction curve plotted with nondimensional coordinates. The results are consistent with the two cases considered by **Steele**, who first reported a numerical solution for a square section.

In paper<sup>18</sup>, the elasto-plastic problem of combined bending and torsion is treated analytically for an incompressible isotropic work-hardening material obeying a nonlinear stress-strain law. Evolving a theory so as to satisfy the equilibrium and compatibility condition, the basic nonlinear differential equation in the ordinal Cartesian coordinate system can be linearized, adopting the new parameter in the stress space.

Provided that **Ramberg-Osgood's** law is employed as a nonlinear stress-strain relation, the linearized basic equation were reduced to the hypergeometric differential equation. Then, the components of strain and corresponding coordinates were described in the form of the hypergeometric series. The numerical calculation was used for the evaluation of the stress components, the bending and twisting moment.

The paper<sup>19</sup> deals with two aspects of work to examine the elastic-plastic behavior of preloaded circular rods subjected to subsequently applied torque within the plastic region.

In the first, uniform diameter and reduced section rods of mild steel, fitted with strain gauges, were subjected to initial axial yield loads using a custom built torque-tension machine, and then holding the initial axial displacements constant, the specimens were gradually twisted. Then the measurements of the resulting torque and load were recorded using appropriate load cells as well as by the fitted strain gauges.

Experimental results with fitted strain gauges show that, even when the axial displacements of the preloaded rods were held constant, the strain gauge readings increase rapidly with the decrease in the initially applied axial loads, as recorded by the appropriate cell, at the confined zone where the plastic deformation begins. Elsewhere of the specimens the strain readings decrease due to elastic recovery of the material.

Secondly, the experimental results thus obtained have been compared with **Brooks** theoretical pre-

dictions, developed for strain-hardening material. Results of elastic-plastic analysis for combined loading were summarized in the book<sup>20</sup>.

### ***Stress & Strain in Naturally Curved & Twisted Solid Bar***

The straight wire in its initial state before coiling of the helical spring is seen in **Figure 2**. The end sections are  $z = 0$  and  $z = L$ . After coiling, the wire turns into a naturally curved and twisted solid bar with circular cross-section  $\Sigma$  of length  $L$ . During coiling, the straight wire is loaded from a stress-free state by terminal bending moment  $M$  and the terminal twist moment  $T$ . Similarly, during preset the helical wire is loaded from a stress-free state by terminal bending moment  $M$  and the terminal twist moment  $T$ . Mathematical analysis for stress and strain in naturally curved and twisted solid bar is given in **Table 3**.

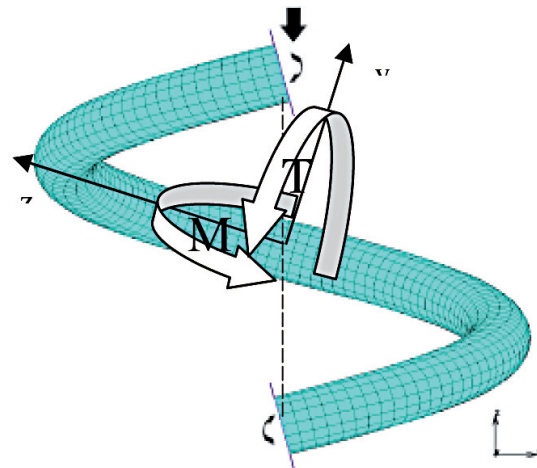


**Fig. 2 — Torsion and bending moments in the cross-section of the spring wire.**

To obtain additional information, contact the author or visit the website listed below.

[www.mubea.com](http://www.mubea.com)

*In Part 2 of this article, to appear in the next issue, the author looks at the theory of elastic-plastic combined bending and torsion of naturally curved and twisted bar, application of combined bending and torsion theory for simulation of preset for helical springs and the conclusions.*

**Table 3 — Stress and strain in naturally curved and twisted solid bar.**

The origin of coordinates is chosen at the centroid of area of one cross-section. The distribution of strain and stress due to above combined loading is independent of the variable  $Z$ . Let the curvature of the axis of cylinder in pure bending is  $K$ . The strain component  $\epsilon_{zz}$  for the naturally curved solid bar can be written as follows

$$(3.1) \quad \epsilon_{zz} = (R^{-1} - R_A^{-1})x = (\kappa - \kappa_A)x, \text{ where } R = 1/K \text{ is radius of curvature of the bar during bending.}$$

We neglect the curvature effects on the stress and strain, assuming that the outer radius of the bar  $r$  is much lower than the curvature radius  $R$  of the bar.

The non vanishing strain components in pure torsion of naturally curved solid bar with circular cross-section of radius  $r$  are the shearing strains

$$(3.2) \quad \gamma_{xz} = 2\epsilon_{xz} = -(\theta - \theta_A)y, \quad \gamma_{yz} = 2\epsilon_{yz} = (\theta - \theta_A)x$$

where  $\theta$  is the angle of twist per unit length of the bar.

We use these relations for description of strains for both straight and initially twisted bars. The only difference between the straight bar and the helical bar is the following. The curvature and the angle of twist of the straight wire vanish, such that  $k_A = 0$ ,  $\theta_A = 0$ .

The in-plane cross-sectional shear strain  $\gamma_{xy} = 2\epsilon_{xy} = 0$  and transversal stress components  $\sigma_{xx} = \sigma_{yy} = 0$

vanish. With these formulas the deformation of the rod is uniquely defined.

The axial and shear deformations in the points

$$x = \rho \sin \varphi, \quad y = \rho \cos \varphi$$

of cross-section for the circular rod are respectively

$$(3.3) \quad \epsilon_{zz}(\rho, \varphi) = (\kappa - \kappa_A)\rho \sin \varphi,$$

$$(3.4) \quad \gamma_{rz}(\rho, \varphi) = \sqrt{\gamma_{xz}^2 + \gamma_{yz}^2} = (\theta - \theta_A)\rho.$$

Maximal axial strain  $\epsilon = \epsilon_{zz}(r, \pi/2) \equiv (\kappa - \kappa_A)r$

and the maximal shear strain  $\gamma = \gamma_{rz}(r, \varphi) \equiv (\theta - \theta_A)r$

attain on the contour of the circular cross-section. Since the strain components are independent of the variable  $Z$ , the strains, stresses and also secant modules are the function of  $\rho, \varphi$  (or  $x, y$ ) only.

If the bending moment  $M = M_p(\kappa - \kappa_A, \theta - \theta_A)$  and torque  $T = T_p(\kappa - \kappa_A, \theta - \theta_A)$  increase proportionally to a single parameter, such that their ratio keeps constant during the plastic deformation, the stress distributions in the cross-section are obtained with the Eqs. (2.5) and (2.6). Using the expression for strains (4.3) and (4.4) in the cross-section, we can calculate stresses during the deformation history.

The bending and torque moments applied to the end sections of the rod are

$$(3.5) \quad M_p = \int_0^{2\pi} \int_0^r \sigma_{zz}(\rho, \varphi) x \rho d\rho d\varphi \equiv \int_0^{2\pi} \int_0^r \sigma_{zz}(\rho, \varphi) \rho^2 \sin \varphi d\rho d\varphi$$

$$(3.6) \quad T_p = \int_0^{2\pi} \int_0^r \tau_{rz}(\rho, \varphi) \rho^2 d\rho d\varphi.$$

Thus, the bending and torque moments could be derived as the functions of curvature  $\kappa - \kappa_A$  and twist  $\theta - \theta_A$  changes of the rod during the plastic deformation.

We analyze the plastic loading with a nonlinear stress strain law. The curvature and twist of the bar during the plastic loading increase proportionally, such that the ratio curvature to twist remains constant.

The integrals (4.5) of bending moment and (4.6) of torsion moment for the cases  $k = 1/2$  and  $k = 1$  are expressed in analytical form:

$$(3.7) \quad M_p(\kappa - \kappa_A, \theta - \theta_A) = \left[ E_\infty + \frac{16}{3\pi}(E - E_\infty)P^{(k)}(\lambda, \mu) \right] (\kappa - \kappa_A)J$$

$$(3.8) \quad T_p(\kappa - \kappa_A, \theta - \theta_A) = \left[ 3\frac{\sqrt{1-\mu^2}}{\mu}G_\infty + \frac{8}{3\pi}(G - G_\infty)Q^{(k)}(\lambda, \mu) \right] \frac{J_p}{\omega}(\kappa - \kappa_A)$$

with  $J_p = 2J = \pi r^4/2$  and  $\epsilon = r\kappa$ .

The following dimensionless parameters are used:

$$\frac{1}{\mu^2} = 1 + \omega^2 \left( \frac{\theta - \theta_A}{\kappa - \kappa_A} \right)^2, \quad \frac{1}{\lambda^2} = \frac{1}{\mu^2} + \left( \frac{\epsilon_p}{\epsilon} \right)^2.$$

The dimensionless functions  $P^{(k)}(\lambda, \mu)$ ,  $Q^{(k)}(\lambda, \mu)$  for the integrable cases are listed below.

## 1.1 HARDENING EXPONENT $k=1/2$

The function  $P^{(1/2)}(\lambda, \mu)$  reads

$$P^{(1/2)}(\lambda, \mu) = p_K^{(1/2)}\mathbf{K}(\lambda) + p_E^{(1/2)}\mathbf{E}(\lambda) + p_\Pi^{(1/2)}\mathbf{\Pi}(\mu^2, \lambda) + p_0^{(1/2)},$$

$$p_K^{(1/2)} = \frac{\sqrt{\mu^2 - \lambda^2}(\lambda^4 - \mu^2)}{\mu\lambda^4},$$

$$p_E^{(1/2)} = \frac{\mu\sqrt{\mu^2 - \lambda^2}}{\lambda^4},$$

$$p_\Pi^{(1/2)} = -\frac{(\mu^2 - \lambda^2)^{5/2}}{\mu\lambda^4},$$

$$p_0^{(1/2)} = \pi \frac{(\lambda^2 - \mu^2)^2}{2\lambda^4 \sqrt{1 - \mu^2}}.$$

Here

$$\mathbf{K}(\lambda) = \int_0^1 \frac{1}{\sqrt{(1 - \lambda^2 t^2)(1 - t^2)}} dt \text{ is the complete Elliptic integrals of the first kind,}$$

$$\mathbf{E}(\lambda) = \int_0^1 \sqrt{\frac{1 - \lambda^2 t^2}{1 - t^2}} dt \text{ is complete elliptic integrals of the second kind,}$$

$$\mathbf{\Pi}(\mu^2, \lambda) = \int_0^1 \frac{1}{(1 - \mu^2 t^2) \sqrt{(1 - \lambda^2 t^2)(1 - t^2)}} dt \text{ is the complete elliptic integrals of the third kind.}$$

The dimensionless function  $Q^{(1/2)}(\lambda, \mu)$  possess the following expression

$$Q^{(1/2)}(\lambda, \mu) = q_K^{(1/2)} \mathbf{K}(\lambda) + q_E^{(1/2)} \mathbf{E}(\lambda) + q_{\Pi}^{(1/2)} \mathbf{\Pi}(\mu^2, \lambda) + q_0^{(1/2)},$$

$$q_K^{(1/2)} = \frac{\sqrt{\mu^2 - \lambda^2} (2\lambda^4 - \lambda^4 \mu^2 - 2\lambda^2 \mu^2 + \mu^4)}{\mu^2 \lambda^4 \sqrt{1 - \mu^2}},$$

$$q_E^{(1/2)} = -\frac{(\mu^2 - \lambda^2)^{3/2}}{\lambda^4 \sqrt{1 - \mu^2}},$$

$$q_{\Pi}^{(1/2)} = \frac{(\mu^2 - 2)(\mu^2 - \lambda^2)^{5/2}}{\lambda^4 \mu^2 \sqrt{1 - \mu^2}},$$

$$q_0^{(1/2)} = \frac{(2 - \mu^2)(\mu^2 - \lambda^2)^2}{2\mu(1 - \mu^2)\lambda^4} \pi.$$

## 1.2 HARDENING EXPONENT $k=1$

The expression  $P^{(1)}(\lambda, \mu)$  reduces to

$$P^{(1)}(\lambda, \mu) = p_1^{(1)} [\Phi(\lambda, \mu) - \Phi(0, \mu)] + p_0^{(1)},$$

$$\Phi(\lambda, \mu) = \arctan \left( \frac{\lambda^2 - 2 + \mu^2}{2\sqrt{1 + \mu^2} \sqrt{1 + \lambda^2}} \right),$$

$$p_1^{(1)} = -\frac{3\pi(\mu^2 + \lambda^2)^2}{8\lambda^4 \sqrt{1 + \mu^2}},$$

$$p_0^{(1)} = \frac{3\pi(\sqrt{1 + \lambda^2} - 1)(\mu^2 + \lambda^2)}{4\lambda^4}.$$

The dimensionless function  $Q^{(1)}(\lambda, \mu)$  is

$$Q^{(1)}(\lambda, \mu) = q_1^{(1)} [\Phi(\lambda, \mu) - \Phi(0, \mu)] + q_0^{(1)},$$

$$q_1^{(1)} = \frac{3\pi\mu\omega(2 - \mu^2)(\mu^2 - \lambda^2)^2}{8\lambda^4(1 + \mu^2)},$$

$$q_0^{(1)} = \frac{3\pi\alpha\mu(-\mu^2\sqrt{1 + \lambda^2} + \mu^2 - \lambda^2)(\mu^2 - \lambda^2)}{4\sqrt{1 + \mu^2}\lambda^4}.$$

These expressions play the fundamental role for the subsequent analysis. With this method we express analytically the bending moment  $M(\kappa, \theta)$  and torque  $T(\kappa, \theta)$  as the functions of curvature of the bar during bending  $\kappa$  and the angle of twist per unit length of the bar  $\theta$ .